

Ascorbate acts as a highly potent inducer of chromate mutagenesis and clastogenesis: linkage to DNA breaks in G₂ phase by mismatch repair

Mindy Reynolds, Lauren Stoddard, Ivan Besselov and Anatoly Zhitkovich*

Department of Pathology and Laboratory Medicine, Brown University, Providence, Rhode Island 02912, USA

Received October 12, 2006; Revised November 3, 2006; Accepted November 8, 2006

ABSTRACT

Here we examined the role of cellular vitamin C in genotoxicity of carcinogenic chromium(VI) that requires reduction to induce DNA damage. In the presence of ascorbate (Asc), low 0.2–2 μ M doses of Cr(VI) caused 10–15 times more chromosomal breakage in primary human bronchial epithelial cells or lung fibroblasts. DNA double-strand breaks (DSB) were preferentially generated in G₂ phase as detected by colocalization of γ H2AX and 53BP1 foci in cyclin B1-expressing cells. Asc dramatically increased the formation of centromere-negative micronuclei, demonstrating that induced DSB were inefficiently repaired. DSB in G₂ cells were caused by aberrant mismatch repair of Cr damage in replicated DNA, as DNA polymerase inhibitor aphidicolin and silencing of MSH2 or MLH1 by shRNA suppressed induction of γ H2AX and micronuclei. Cr(VI) was also up to 10 times more mutagenic in cells containing Asc. Increasing Asc concentrations generated progressively more mutations and DSB, revealing the genotoxic potential of otherwise nontoxic Cr(VI) doses. Asc amplified genotoxicity of Cr(VI) by altering the spectrum of DNA damage, as total Cr-DNA binding was unchanged and post-Cr loading of Asc exhibited no effects. Collectively, these studies demonstrated that Asc-dependent metabolism is the main source of genotoxic and mutagenic damage in Cr(VI)-exposed cells.

INTRODUCTION

Occupational exposure to chromium(VI) has long been recognized as a carcinogenic factor for the lung and other respiratory tissues (1,2). Approximately 360 000 workers in the US and several million worldwide are currently exposed to Cr(VI) in the workplace. Frequent environmental contamination with this metal has raised significant health concerns for

several non-industrial populations, particularly for those with drinking water contamination or residing in close proximity to large sites of chromate disposal (3,4). However, it has also been argued that detoxification processes should limit cancer risk to the cases of massive occupational exposures (5). Carcinogenic potential of Cr(VI) is supported by its ability to cause DNA damage and mutations, although its mutagenicity has been found to be modest and typically detected at very toxic doses (6). Recent epidemiological and risk assessment studies conducted by the EPA have found ~25% lifetime risk of dying of lung cancer under the current permissible exposure limit (PEL) (7,8). These findings served as the basis for the OSHA decision in early 2006 to lower the PEL for Cr(VI) by 10-fold (9). Even under the new standard, a lifetime exposure was estimated to cause 10–45 additional lung cancers per 1000 workers. This strikingly high cancer risk for Cr(VI) exposures experienced by hundreds of thousands of people requires a much better understanding of the mechanisms of high Cr(VI) genotoxicity and adequate approaches to assess it. Weak mutagenicity and the need for relatively high doses for the induction of other genotoxic responses were clearly inconsistent with the very strong carcinogenic potential of Cr(VI).

Cr(VI) is a pro-carcinogen that generates DNA damaging species via its reductive activation in cells by ascorbate (Asc) and small thiols, such as cysteine and glutathione (10). While the final product of all reduction reactions is always Cr(III), there are very important differences in reduction rates and the nature of intermediate products. Reduction of Cr(VI) by thiols is relatively slow and produces transient Cr(V) and Cr(IV) species, whereas reaction with the two-electron donor Asc is fast and generates Cr(IV) as the main intermediate (10,11). Metabolism of Cr(VI) by Asc and thiols also yields different spectra of ternary Cr-DNA adducts (10). The formation of Cr(V) intermediates have been frequently considered an important indicator of the genotoxic consequences due to its ability to catalyze Fenton-like redox reactions (12) and, in some ligand environments, to cause direct DNA oxidation (13,14). However, there has been some technical bias for studies with Cr(V) because, unlike Cr(IV), several relatively stable Cr(V) complexes could be synthesized allowing examination of their genotoxic and chemical

*To whom correspondence should be addressed. Tel: +1 401 863 2912; Fax: +1 401 863 9008; Email: anatoly_zhitkovich@brown.edu

properties. Considering that Asc is a dominant reducer of Cr(VI) in tissues (15) and does not directly generate Cr(V) at physiological conditions (16,17), then one would predict that only a rapid inflow of massive Cr(VI) doses resulting in a severe drop in Asc levels could cause significant Cr(V) production and DNA damage. The causes for increased Cr(V) formation under these conditions would include a shift to thiol-dependent metabolism and increased stability of Cr(IV) intermediates that can generate Cr(V) via secondary reactions (10). However, the hypothesis on the overriding importance of Cr(V) is not supported by studies on the formation of mutagenic damage *in vitro* (18) and the fact that Cr(VI) is a weak mutagen in mammalian cells (6) that rely on thiols to reduce Cr(VI) due to scarcity of cellular Asc in the standard tissue cultures (10,19).

In this work, we examined the importance of cellular Asc in the manifestation of the genotoxic abilities of Cr(VI). We found that metabolism of Cr(VI) by cellular Asc caused dramatic increases in the formation of chromosomal damage and mutations at the endogenous *Hprt* gene. Mechanistically, increased DNA breakage was associated with abnormal processing of Cr-DNA damage by the mismatch repair (MMR) machinery of cells entering G₂ phase.

MATERIALS AND METHODS

Cells and exposures

Primary human lung IMR90 fibroblasts were obtained from ATCC and typically used at passage 6–9. Primary human bronchial epithelial (HBE) cells were purchased from Clonetics and used at passage 4–6. All treatments with potassium chromate (Cr(VI)) were performed in serum-free media for 3 h. HBE cells were treated with Cr(VI) in RPMI1640 medium supplemented with growth factors. Loading with Asc was done by incubating cells for 90 min with dehydroascorbic acid (DHA) in either Krebs-HEPES buffer supplemented with 0.5 mM glucose (IMR90, V79 and CHO cells) or standard basal epithelial growth medium (HBE cells). The following DHA concentrations were used: 5 mM for IMR90; 50, 200 and 500 μ M for HBE; 0.5, 1 and 2 mM for V79; and 2 mM for CHO cells. In experiments with arrested S-phase progression, 1 μ M aphidicolin was added 15 min before Cr(VI) and was present during Cr exposure and post-exposure incubations. Control cells were incubated with equivalent concentrations of DMSO.

Asc measurements

Cellular Asc was measured by a modified HPLC procedure based on the detection of a specific conjugate with 1,2-diamino-4,5-dimethoxybenzene dihydrochloride (DDB) (19). Cells were collected by trypsinization and washed three times in cold PBS (1100 g for 5 min at 4°C). Cell pellets were resuspended in 50 μ l of ice-cold deionized H₂O followed by the addition of 50 μ l of 100 mM methanesulfonic acid containing 10 mM diethylenetriaminepentaacetic acid. Cells were lysed by two cycles of freezing (–80°C) and thawing (37°C). Asc-containing supernatants were obtained after centrifugation at 12000 g for 10 min at 4°C. Aliquots of each sample (typically 10 μ l) were mixed with 90 μ l of a

dye solution containing 0.2 units/ μ l Asc oxidase, 50 mM sodium acetate (pH 6.2), and 0.5 mM DDB and incubated for 4 h at room temperature in dark. Chromatographic separation was performed on Beckman Coulter Ultrasphere column (ODS 5 μ m, 4.6 mm \times 250 mm) employing isocratic elution with 75% 50 mM phosphoric acid (pH 2.0) and 25% acetonitrile for 20 min. DHA-DDB conjugate was detected by its characteristic fluorescence (458 nm emission and 371 nm excitation). HPLC analyses were performed with a Shimadzu LC-10ADvp liquid chromatograph, equipped with a SIL-10ADvp autosampler and an RF-10AxL fluorescence detector. The detection limit for cellular Asc was 0.1 μ M.

Chromium analyses

All Cr measurements were performed using graphite furnace atomic absorption spectroscopy employing Zeeman background correction (Perkin-Elmer GF-AAS, model 41002L). Instrumentation settings were as described previously (19). Cellular Cr content was measured using nitric acid-prepared extracts (20). For quantitation of Cr-DNA adducts, DNA was isolated by a phenol-chloroform procedure omitting EDTA (19). The detection limit was 0.4 pmol chromium or 1 Cr adduct per 10000 nt.

Microscopy

Cells were grown on Superfrost Plus slides, loaded with Asc, exposed to Cr(VI) for 3 h and returned to complete medium. Bromodeoxyuridine (BrdU) labeling was performed by incubation with 10 μ M of a cell proliferation labeling reagent (Amersham) for 15 min in the dark prior to Cr exposure. At the indicated times, cells were washed twice with PBS, fixed with 2% paraformaldehyde in PBS for 15 min and permeabilized with 1% Triton X-100 for 15 min at room temperature. For micronuclei scoring, slides were blocked for 1 h in 5% goat serum at room temperature. Slides were then incubated with anti-centromere CREST antibody (Antibodies, Inc.) at 1:200 dilution for 2 h at 37°C in a humidified chamber followed by incubation with the secondary Alexa-Fluor 488-conjugated anti-human IgM antibody for 1 h. Nuclei were counterstained with 4'-6'-diamidino-2-phenylindole (DAPI) and mounted with Vectashield hard set mounting medium (Vector Laboratories). Micronuclei were scored from fluorescence images recorded using a Nikon Eclipse E800 digital microscope. At least 500 cells were analyzed for each slide. For all other immunostainings, slides were incubated with 2% FBS for 30 min at 37°C in a humidified chamber. Double labeling was performed by simultaneous incubation of primary antibodies for γ H2AX at 1:150 (Upstate), anti-53BP1 at 1:200 (Santa Cruz), anti-BrdU at 1:100 (PharMingen), or anti-cyclin B1 at 1:200 (Santa Cruz) dilutions for 2 h at 37°C in a humidified chamber. Slides were washed three times with PBS for 5 min followed by incubation with Alexa-Fluor 488-conjugated anti-mouse IgG and Alexa-Fluor 594 or 564-conjugated anti-rabbit IgG secondary antibodies (Molecular Probes) for 1 h at room temperature. All antibodies were diluted in 2% bovine serum albumin (BSA), with the exception of anti-BrdU staining solution, which additionally contained 1 mM MgCl₂ and 125 U/ml Benzonase nuclease (Novagen). Slides were washed four times with PBS for 5 min and mounted with

Vectashield hard set mounting medium containing DAPI (Vector Laboratories). Fluorescence images were recorded with a Zeiss Axiovert 100 confocal microscope and analyzed by Phoenix and Metamorph software. Experiments were repeated three to four times with at least 100 cells analyzed on each slide. Slides were always coded and scored in a blind manner.

Stable small interfering RNA knockdowns

Stable downregulation of MLH1 or MSH2 was achieved by infections with a pSUPER-RETRO retroviral vector encoding a hairpin forming small interfering RNA (siRNA). For construction, the pSUPER-RETRO plasmid was linearized with HindIII and BglII to allow for insertion of the annealed oligonucleotides directed towards the mRNA of interest.

MLH1 oligos were 5' gatccccggctcactactagtaaaccttcaaga-gaagttactagtagtgaaaccttttgaaa and 5' agctttccaaaaggttcac-tactagtaaaccttcttgaaagttactagtagtgaaaccggg [design based on Ref. (21)].

MSH2 oligos were 5' gatccccgagtgttgcttagtaaatcaaga-gattactaagcacaactcttttgaaa and 5' agctttccaaaagagtgttg-tgcttagtaaatctcttgaaattactaagcacaactcggg.

Oligonucleotides targeting luciferase were used as a control:

5' gatccccgcgaccaacgccttgattgttcaagagacaatcaaggcgttgct-gcttttgaaa and 5' agctttccaaaagcgaccaacgccttgattgtctt-gaacaatcaaggcgttgctcggg. The pSUPER-RETRO vectors were transfected into 293 cells with plasmids encoding viral packaging proteins (22) using Plus reagent and Lipofectamine (Invitrogen) according to the manufacturer's instructions. Two days post-transfection, medium containing virus particles was added to IMR90 cells and infections were allowed to proceed for 24 h. Vector-expressing cells were selected seven days post infection in the presence of 1.5 µg/ml of puromycin.

Western blotting

Protein extracts were prepared using a lysis buffer freshly supplemented with protease and phosphatase inhibitors [50 mM Tris (pH 8.0), 250 mM NaCl, 1% NP-40, 0.1% SDS, 5 mM EDTA, 2 mM Na₃VO₄, 10 mM Na₂P₂O₇, 10 mM NaF, 10 µg/mL aprotinin, 10 µg/mL leupeptin, 0.5 µg/mL pepstatin, and 1 mM PMSF]. Cells were incubated on ice for 10 min and then cell debris was spun down at 10000 g for 10 min. Proteins were separated by SDS-PAGE and electrotransferred to ImmunoBlot PVDF membrane (BioRad). Anti-MLH1 and anti-MSH2 (PharMingen) primary antibodies were used. Protein bands were visualized using horseradish peroxidase-conjugated secondary antibodies (Upstate) and enhanced chemiluminescence kit (Amersham).

Mutagenesis

V79 and CHO cells were routinely maintained in DMEM-10%FBS and MEM-10%FBS media, respectively. Standard media for both cell lines were supplemented with HAT mixture (Invitrogen) for 7–9 days prior to seeding for Cr exposures. Cells were seeded (0.5×10^6 cells) on 100 mm dishes and allowed to attach overnight. Cells were then loaded with Asc, exposed to Cr(VI) for 3 h, returned to complete medium, and cultured for 7 days to allow expression of

the *Hprt*^{-/-} phenotype. Cells were reseeded in medium containing 40 µM 6-thioguanine (6-TG) at a density of 0.5×10^6 cells per 100 mm dish. The plating efficiency (clonal survival) in the nonselective medium was also determined. Ten to fourteen days after seeding, colonies were stained with Giemsa solution and counted. Mutation frequency was calculated by dividing the number of 6-TG resistant colonies per 10^6 clonable cells.

RESULTS

Asc is a potent activator of DNA double-strand breaking and clastogenic activities of Cr(VI)

We have previously noted that several transformed human cells had very low or undetectable cellular Asc (19). Even when freshly fed cells initially contained detectable amounts of Asc (20–50 µM), it was lost during the next 1–2 days in culture (23). To test whether primary human cells are also Asc-deficient, we measured Asc concentrations in IMR90 lung fibroblasts using a highly sensitive HPLC assay (19). We found that one day after seeding, IMR90 cells contained barely detectable amounts of Asc (2.8 ± 1.1 µM, $n = 4$) (Figure 1A). To restore normal levels of Asc, we incubated cells with DHA, which rapidly enters cells and is then reduced to Asc (24). Loading of cells with Asc directly is very inefficient (19,25) and is usually associated with oxidative stress and toxic effects caused by extracellular reactions (25). Incubation of IMR90 fibroblasts with 5 mM DHA created 1 ± 0.2 mM ($n = 4$) intracellular Asc, which was comparable to Asc levels in freshly purified human lymphocytes (Figure 1A).

The effect of cellular Asc on the genotoxic potential of Cr(VI) was first examined by scoring cells containing foci of Ser-139 phosphorylated H2AX (γ H2AX), which are specific quantitative markers of DNA double-strand breaks (DSB) (26,27). We found that preloading with Asc greatly increased the ability of low doses of Cr(VI) to cause γ H2AX foci in IMR90 cells (Figure 1C). In the linear response range (0–2 µM Cr), Asc increased the yield of γ H2AX-containing cells by 5-fold. Enhanced formation of DNA breaks in Asc-containing cells was observed at multiple time points after Cr exposure although it appeared to be more pronounced at earlier times (Figure 1D). Irrespective of their Asc status, the majority of cells with γ H2AX foci stained for G₂ phase marker cyclin B1 (Figure 1B). The percentage of γ H2AX+ cells expressing cyclin B1 in Asc-containing samples was 75.6, 76.5, 73.6 and 92.7 for 1, 3, 6 and 12 h after exposure to 3 µM Cr(VI). The corresponding values for Asc-free cells were 46.7, 68.4, 71.4 and 77.1%. An apparent decrease in the relative yield of γ H2AX+ cells at the high Cr dose (Figure 1C) therefore probably reflected limited amounts of G₂ cells (typically 14–16% for IMR90). Staining for γ H2AX was not due to apoptotic DNA breaks because addition of the validated antiapoptotic dose of 50 µM Z-VAD-FMK pancaspase inhibitor had no effect on the percentage of Asc-containing cells with γ H2AX foci ($10.1 \pm 1.2\%$ without and $10.2 \pm 0.8\%$ with Z-VAD for 2 µM Cr at 6 h post-exposure; $14.2 \pm 2.8\%$ versus $13 \pm 2.9\%$ at 18 h).

To assess the levels of unrepaired DSB, we scored the number of cells with micronuclei (28,29). Treatment with

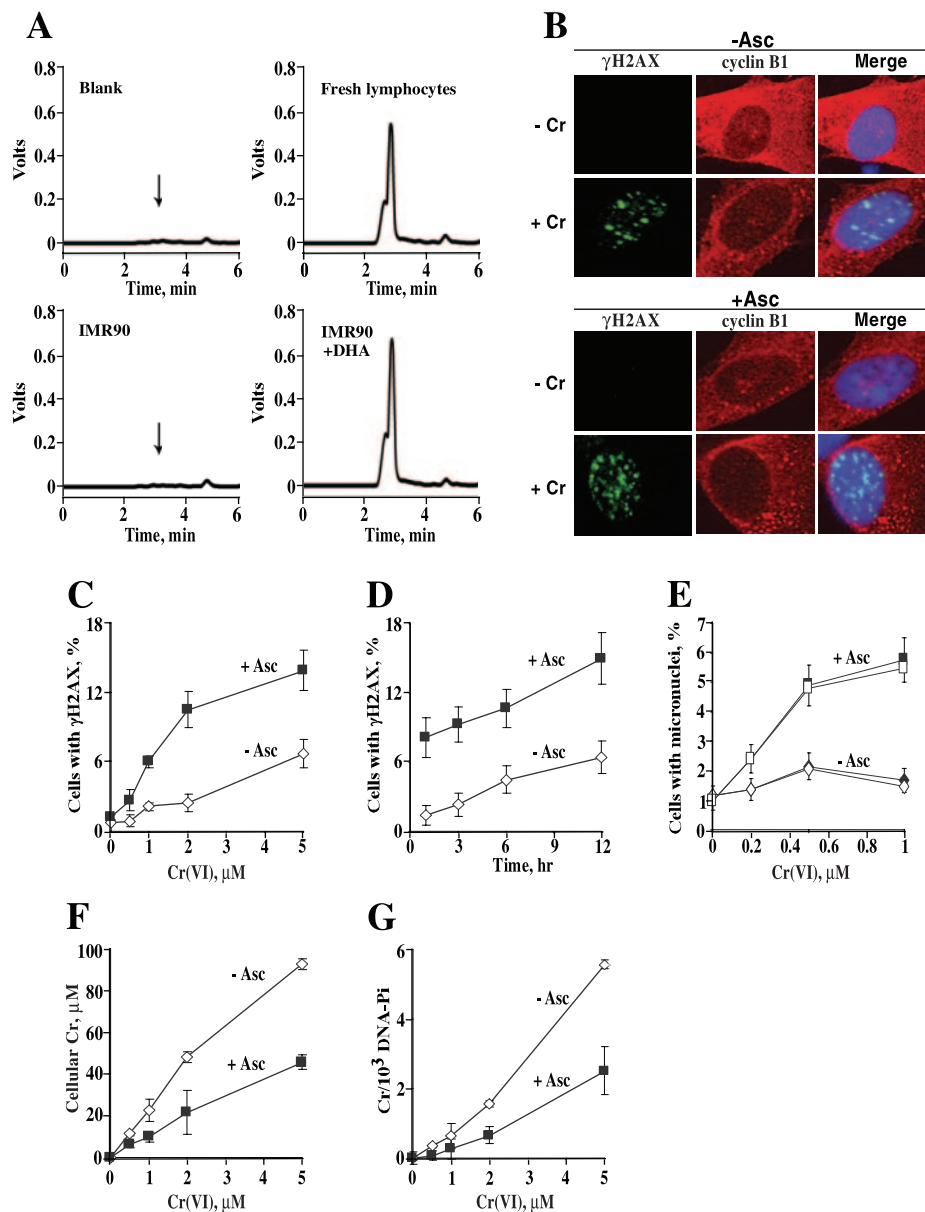


Figure 1. Increased genotoxicity of Cr(VI) in IMR90 cells containing Asc. (A) Representative HPLC profiles for Asc determinations in protein-normalized extracts. (B) Confocal images of IMR90 cells immunostained for γ H2AX, cyclin B1 and counterstained with DAPI. Control or 1 mM Asc-loaded cells were treated with 2 μ M Cr(VI) for 3 h and fixed 6 h later. (C) Preloading with 1 mM Asc increased the number of cells with γ H2AX foci at different Cr doses and (D) times after exposure. Dose-dependence was measured at 6 h post-exposure and time-dependence was determined with 3 μ M Cr(VI). Cells with four or more foci were defined as positive. Results are means \pm SD for at least four slides with >100 cells scored per slide. Data in panel D are after subtraction of background values in Cr-untreated samples (1.9 \pm 0.7 and 1.6 \pm 0.6 for Asc- and Asc+ samples, respectively). (E) Elevated frequency of micronuclei in cells loaded with 1 mM Asc prior to Cr(VI) exposure. Micronuclei were scored 48 h after Cr exposure. Closed symbols—total micronuclei, open symbols—CREST-negative micronuclei. Data are means \pm SD for four slides with >500 cells counted per slide. (F) Cells preloaded with 1 mM Asc had lower uptake of Cr(VI) and (G) lower Cr-DNA binding. Results are means \pm SD for 3–5 independent samples.

low 0.2–1 μ M doses of Cr(VI) strongly induced the formation of micronuclei in Asc-loaded IMR90 cells whereas the responses in Asc-deficient cells were very small if any (Figure 1E). On average, cellular Asc increased the yield of micronuclei by 6.6-fold. Cr-induced micronuclei resulted primarily from clastogenic events (chromosomal breaks) because the majority of them were negative for staining with anti-kinetochore CREST antibody (Figure 1E). One reason for the highly elevated genotoxicity of Cr(VI) by cellular Asc could have been enhanced Cr(VI) accumulation

and/or increased formation of Cr-DNA adducts. However, we found that both Cr(VI) uptake and Cr-DNA binding were in fact lower in Asc-loaded IMR90 cells by 2.1- and 2.3-fold, respectively (Figure 1F and G). We traced the diminished Cr loading to the leakage of cellular Asc, which led to the reduction of Cr(VI) outside the cell. After normalization for the differences in uptake, the presence of 1 mM Asc in IMR90 cells increased the levels of Cr(VI)-induced DSB by 10.5-fold and the number of micronuclei by 13.9-fold.

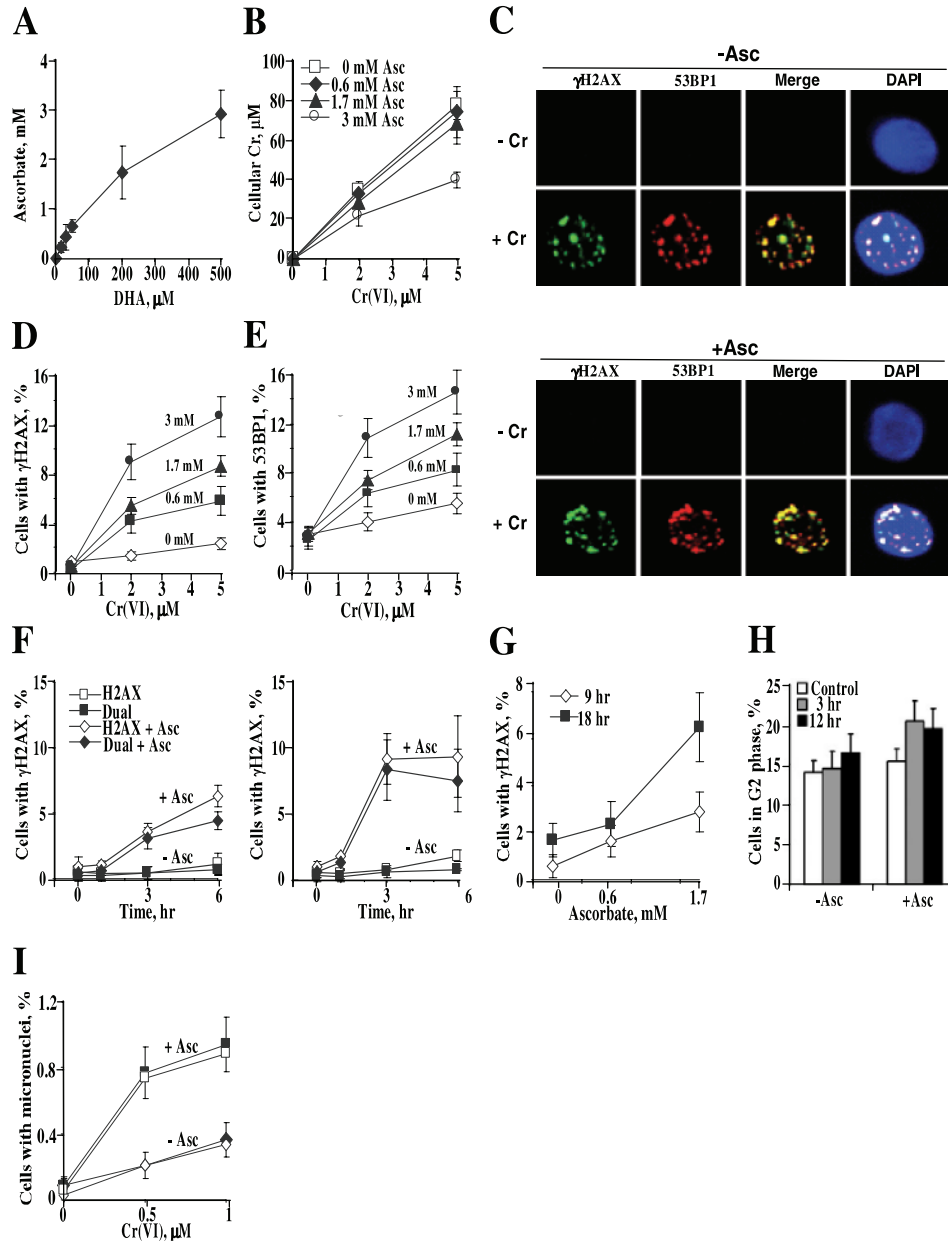


Figure 2. Asc caused concentration-dependent increases in DSB foci and micronuclei in primary HBE cells. (A) Accumulation of Asc by HBE cells. Data are means \pm SD for six independent samples. (B) Cr(VI) uptake by HBE cells containing different Asc concentrations. Data are means \pm SD for four independent samples. (C) Confocal images of cells immunostained for γ H2AX, 53BP1 and counterstained with DAPI. Control and preloaded with 1.7 mM Asc-cells were treated with 2 μ M Cr(VI) for 3 h and fixed 6 h later. (D) Preloading with Asc increased the number of cells containing foci of γ H2AX and (E) 53BP1. Slides were fixed for immunostaining at 6 h after Cr treatment. Cells containing ≥ 4 foci were scored as positive. Data are means \pm SD for four to eight slides with >100 cells counted per slide. (F) Asc-promoted γ H2AX foci were preferentially formed in cells expressing a G₂ phase-specific marker cyclin B1. Cells lacking or containing 1.7 mM Asc were treated with 2 μ M Cr(VI) (left panel) or 5 μ M Cr(VI) (right panel). H2AX—percentage of γ H2AX+ cells, dual—percentage of cells that are positive for both γ H2AX and cyclin B1. Data are means \pm SD for four slides with >100 cells/slide. (G) Physiological but not low levels of Asc caused delayed induction of γ H2AX after exposure to subtoxic 0.5 μ M Cr(VI). Foci were scored at 9 and 18 h after Cr treatment of cells containing 0, 0.6 or 1.7 mM Asc. Results are means \pm SD for four slides with >450 cells counted. Data are after subtraction of background values in Cr-untreated samples (9 h: 0.7 \pm 0.5, 1.6 \pm 1.2 and 1.4 \pm 1.2%; 18 h: 0.4 \pm 0.8, 0.2 \pm 0.4 and 0.5 \pm 0.5% for 0, 0.6 and 1.7 mM Asc samples, respectively). (H) Percentage of G₂ cells detected by positive immunostaining for cyclin B1. Cells with (1.7 mM) and without Asc were treated with 2 μ M Cr(VI) and fixed for immunofluorescence at 3 and 12 h post-exposure. Data are means \pm SD for three slides with >100 cells/slide counted. (I) Preloading with Asc (1.7 mM) increased the induction of micronuclei by Cr(VI). Results are means \pm SD for eight slides with >1000 cells/slide counted. Closed symbols—total micronuclei, open symbols—CREST-negative micronuclei.

To further verify our observations, we examined DSB-related foci formation in primary HBE cells. These cells were grown in synthetic medium without serum and had no detectable Asc. Loading of HBE cells with Asc was highly efficient even using low concentrations of DHA (Figure 2A).

The presence of 0–1.7 mM cellular Asc had only a minor effect on Cr(VI) accumulation (Figure 2B), which permitted easier testing of Asc dose-dependence. We found that even the subphysiological concentration of 0.6 mM Asc caused a major increase in formation of γ H2AX foci in HBE cells at

6 h post-Cr exposure (Figure 2D). Cells with physiological 1.7 and 3 mM Asc were even more susceptible to DSB induction. Analysis of another quantitative marker of DSB, 53BP1 foci (30), also revealed highly elevated levels of DSB in Asc+ cells treated with Cr (Figure 2E). 53BP1 is recruited to DSB prior to Ser-139 phosphorylation of H2AX (31) and independently of any other DSB-responsive proteins (32). The magnitude of increase in γ H2AX and 53BP1 foci by 3 mM Asc was particularly striking because these cells had significantly lower uptake of Cr(VI) (Figure 2B). For 2 μ M Cr(VI) exposures, cells without Asc had no changes in γ H2AX foci whereas preloading with 1.7 and 3 mM Asc led to 7.5 and 20-fold increases above untreated controls, respectively. All γ H2AX+ cells invariably contained 53BP1 foci and the majority of γ H2AX and 53BP1 foci colocalized (Figure 2C). Approximately 3% of control cells contained 53BP1 foci but no γ H2AX foci and this fraction of cells remained constant irrespective of any Asc or Cr manipulations. In contrast to the frequency of foci+ cells, Asc had no impact on the number of DSB foci per foci-positive cell. For example, 5 μ M Cr(VI) treatments induced 11.3 versus 12.2 γ H2AX foci/cell and 15.6 versus 16.3 53BP1 foci/cell for no Asc and 1.7 mM Asc-containing HBE cells, respectively (6 h post-Cr analyses). Examination of other post-exposure times and lower Cr doses also failed to detect any significant differences in the number of γ H2AX foci per positive cell between Asc+ and Asc- samples (e.g. for 2 μ M Cr: 11.7 versus 10.3 at 3 h and 12.8 versus 11.9 foci/cell at 12 h for 1.7 mM Asc-loaded and no Asc samples, respectively). These results suggested that the main effect of Asc was manifested in the increased fraction of cells susceptible for DSB induction, not in the increased amount of DNA damage. This interpretation is also consistent with the observed independence of Cr-DNA binding on the presence of Asc (Figure 2B).

Time-course studies showed that Asc-promoted DSB did not appear until 3 h post-Cr exposure and either leveled off (5 μ M Cr) or continued to increase at 6 h (2 μ M Cr) (Figure 2F). Data collected at 6 h post-Cr revealed an upward trend but not a major increase in DSB foci for cells with 1.7 versus 0.6 mM Asc (Figure 2D and E), which could have been a result of a particular combination of Cr doses and timing. To further investigate potential differences between normal and subphysiological Asc levels, we studied DSB formation at longer post-exposure times using a very low dose of 0.5 μ M Cr(VI). We found that the presence of physiological 1.7 mM Asc did cause increased processing of Cr-DNA damage into DSB, which became clearly evident at 18 h after exposure (Figure 2G). We found that 80–95% of DSB were induced in G₂ phase as detected by dual staining of γ H2AX and cyclin B1 (Figure 2F). However, not all G₂ cells were susceptible to DSB induction, as the number of cyclin B1+ cells exceeded the number of γ H2AX+ cells, particularly for lower Cr doses and early times (compare Figure 2H versus Figure 2F, left panel). While Asc alone had no effect on the size of the G₂ population, its presence induced detectable increases in the percentage of G₂ cells after Cr exposure (Figure 2H). This modest alteration in cell cycle distribution probably resulted from a delayed progression of DSB-containing G₂ cells into mitosis.

To test whether DSB generated by low levels of Cr damage had clastogenic consequences, we scored the number of micronuclei in control and 1.7 mM Asc-preloaded cells. We found that cellular Asc strongly promoted the formation of micronuclei following Cr(VI) treatments (Figure 2I). At 0.5 μ M Cr(VI), the number of micronuclei in Asc-loaded cells was 13-times above untreated controls whereas Asc-free cells showed only a marginal response. About 95% of Cr-induced micronuclei lacked kinetochores (CREST-negative), indicating clastogenic mechanism of their formation.

Asc is a potent enhancer of Cr(VI) mutagenicity

Next, we examined the effects of cellular Asc on Cr(VI) mutagenicity at the *Hprt* locus in two standard test lines, CHO and V79 (33). Control experiments have shown that preloading of CHO cells with 1.4 mM Asc led to 2.6-times lower Cr(VI) accumulation (Figure 3A) and decreased Cr-DNA binding (Figure 3B). The diminished number of Cr-DNA adducts in Asc+ cells was a direct result of lower Cr accumulation, as evidenced by essentially identical plots of Cr-DNA adducts versus intracellular Cr concentrations (Figure 3C). To correct for the observed uptake differences, we therefore analyzed mutagenic responses as a function of cellular Cr doses (Figure 3D). We found that 0–220 μ M cellular Cr(VI) doses were non-mutagenic in control CHO cells containing 15 μ M Asc. In contrast, preloading of these cells with 1.4 mM Asc caused a strong, linear increase in the frequency of *Hprt* mutants, which reached a 19.2-fold increase over background for the highest Cr dose. The presence of Asc also increased clonogenic lethality of Cr in CHO cells (Figure 3E), although the differences in toxicity were significantly less pronounced than for the mutagenic responses. Cr(VI) mutagenicity was also enhanced by Asc in a concentration-dependent manner at the *Hprt* locus of V79 cells (Figure 3G). While treatment of control V79 cells with 10 μ M Cr(VI) produced only a marginal increase in the number of *Hprt* mutants, the same dose of Cr caused progressively greater mutagenic responses in cells preloaded with increasing Asc concentrations, yielding almost 10 times more mutants for 3.4 mM Asc-containing cells relative to control cells. Uptake studies showed that loading of V79 cells with Asc had either no effect or only a modest, 25% decrease for 3.4 mM Asc samples (Figure 3F). Lack of mutagenic responses in Asc-deficient CHO cells treated with mildly toxic doses of Cr(VI) did not mean that Cr(VI) was completely non-mutagenic in the absence of vitamin C. We found that when the cellular dose of Cr was raised to 0.45 mM, this induced a significant, 3.8-fold increase (SD = 1.0, *n* = 4) in the number of *Hprt* mutants in Asc-deficient CHO populations.

Potentiating effects of Asc result from its effects on metabolism of Cr(VI)

Increased genetic damage due to cellular Asc can result from the changes in the types of DNA lesions and/or altered cellular responses to the same Cr-DNA damage. To evaluate these possibilities, we examined genotoxic and mutagenic responses in cells loaded with Asc 1 h after Cr treatments. This time interval is sufficient for the completion of Cr(VI) reduction in Asc-free cells (34,35). We found that the post-Cr delivery of Asc had no detectable effect on the

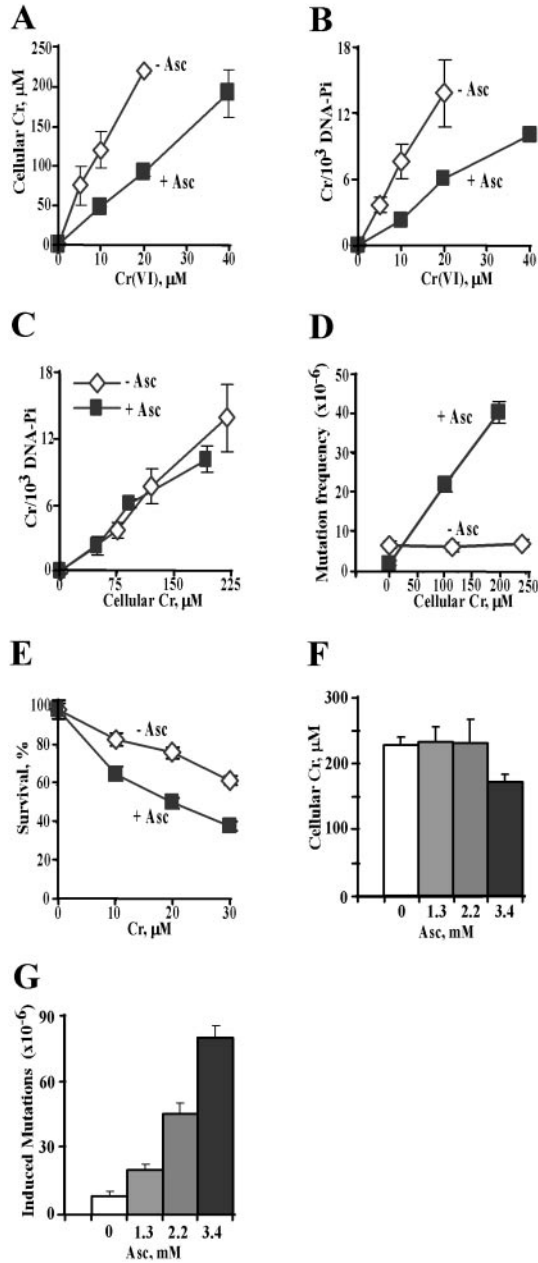


Figure 3. Cellular Asc strongly increases mutagenicity of Cr(VI). (A) Cr uptake and (B) Cr-DNA binding in control (15 μM Asc) and Asc-preloaded (1.4 mM) CHO cells. Means ± SD for 3–6 independent samples. (C) Yield of Cr-DNA adducts in CHO cells as a function of intracellular Cr dose. (D) Frequency of *Hprt* mutants in control (15 μM Asc) and Asc-preloaded (1.4 mM) CHO cells. Cells were treated with 0–40 μM Cr(VI). Mutation frequencies are means±SD for four independent populations. (E) Clonogenic survival of control and 1.4 mM Asc-containing CHO cells. Data are means ± SD from two clonogenic assays with triplicate dishes. (F) Cr uptake (means ± SD, *n* = 4) and (G) Cr-induced *Hprt* mutagenesis in V79 cells containing different concentrations of Asc. Cells were exposed to 10 μM Cr(VI). Data are means ± SD for 4–8 independently treated populations. Background frequencies were 3.6×10^{-5} for control (0.8 μM Asc), 3.4×10^{-5} for 1.3 mM, 3.9×10^{-5} for 2.2 mM and 2.8×10^{-5} for 3.4 mM Asc-containing cells.

formation of micronuclei in IMR90 fibroblasts, the number of γH2AX-containing HBE cells or *Hprt* mutagenesis in CHO cells (Figure 4A–C). These results clearly demonstrate that Asc does not change biological responses to Cr-DNA

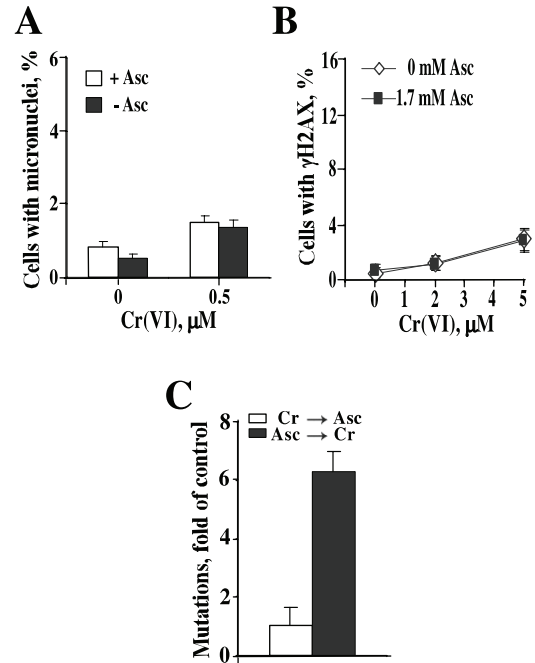


Figure 4. Post-exposure loading of Asc had no effect on genotoxicity and mutagenicity of Cr(VI). Asc was loaded into cells 1 h after Cr(VI) exposure. (A) Formation of micronuclei in IMR90 cells. (B) Frequency of γH2AX foci-containing HBE cells and (C) *Hprt* mutagenesis in CHO cells. CHO cells were loaded with 1.4 mM Asc either before (Asc→Cr) or 1 h after (Cr→Asc) exposure to 10 μM Cr(VI). Results are means ± SD.

damage that is already formed. Therefore, the potentiating abilities of Asc must stem from the altered metabolism of Cr(VI) and resulting changes in the spectrum of DNA lesions.

Suppression of clastogenic responses by downregulation of MSH2 and MLH1 MMR proteins

Here we investigated whether amplification of clastogenic damage by Asc was a direct result of the formation of highly toxic DNA lesions or if it was caused by stronger cellular responses to Asc-mediated Cr-DNA damage. We focused our attention on the potential role of MMR proteins as they have recently been found to enhance genotoxic responses in human colon cancer cells treated with Cr(VI) under standard tissue culture conditions (36). To create deficiency in primary MMR human cells, we infected IMR90 fibroblasts with retroviral constructs expressing short hairpin (sh)RNA targeting MSH2 and MLH1. Both MSH2 and MLH1 are essential MMR proteins and the loss of either protein causes complete MMR deficiency (37,38). The shRNA-expressing vectors were very effective and decreased amounts of MLH1 and MSH2 proteins to barely detectable levels (Figure 5A). Depletion of either MLH1 or MSH2 dramatically suppressed the frequency of micronuclei induced by Cr(VI) in both Asc+ (Figure 5B) and Asc– cells (Figure 5C). For low Cr-DNA damage induced by 0.5 μM Cr(VI), loss of MMR proteins led to a complete abrogation of clastogenic events detected by the micronucleus assay. To explore a potential link between MMR-induced micronuclei and DSB, we also analyzed formation of γH2AX in the same Cr dose range (0–1 μM Cr) as a function of MLH1 and MSH2 status. We

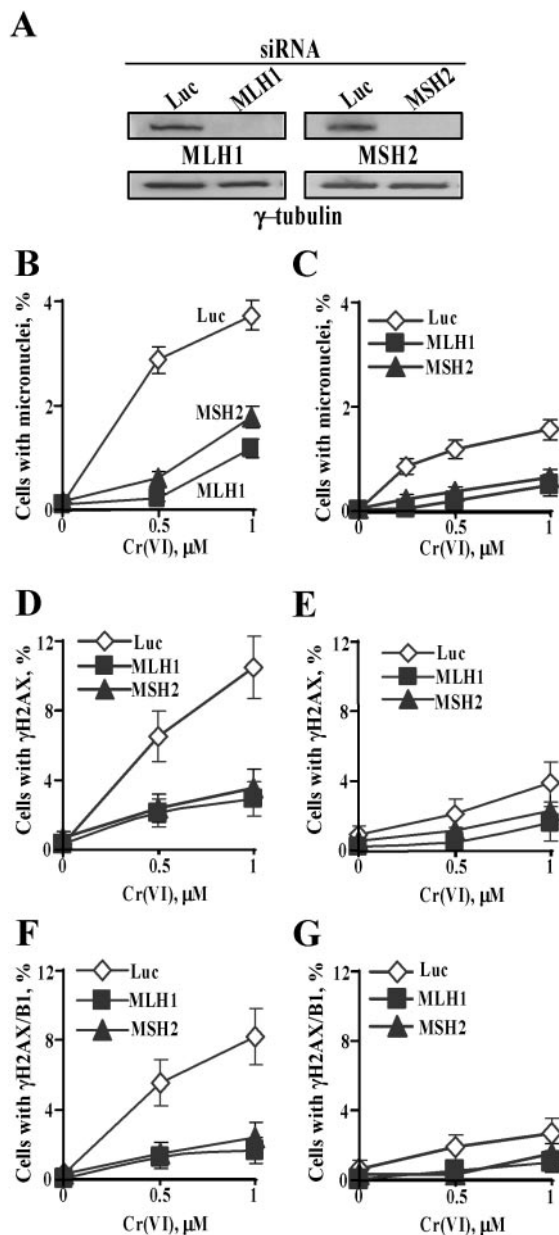


Figure 5. Suppression of γ H2AX and micronuclei formation by stable downregulation of MLH1 and MSH2 proteins. (A) Western blots for MSH2 and MLH1 in IMR90 cells expressing targeting (MLH1, MSH2) and non-specific (Luc) shRNA. Frequency of micronuclei in IMR90 cells (B) preloaded with 1 mM Asc (C) in Asc-deficient cells. Data are means \pm SD for four slides with >1000 cells counted per slide. Induction of γ H2AX by Cr(VI) in cells (D) containing 1 mM Asc and (E) lacking Asc. Slides were fixed for immunofluorescence at 18 h post-Cr. Data are means \pm SD for four slides with >200 cells/slide counted. Frequency of γ H2AX/cyclin B1 double positive cells in (F) Asc-loaded and (G) Asc-deficient samples. Experimental conditions were as in panels (D) and (E).

found that knockdowns of MLH1 and MSH2 proteins also strongly decreased the number of γ H2AX+ cells in both Asc+ (Figure 5D) and Asc- populations (Figure 5E). Suppression of MMR essentially eliminated the formation of DSB in G₂ cells, as evidenced by almost complete absence of γ H2AX/cyclin B1 double positive cells (Figure 5F and G). Overall, these results strongly link MMR to the induction of DSB and micronuclei in Cr-treated cells.

Formation of γ H2AX in G₂ phase requires passage of cells through S-phase

The observed G₂-selectivity in DSB induction was clearly not a result of some intrinsic susceptibility of all G₂ cells since the percentage of γ H2AX+ cells was significantly lower than the total number of G₂ cells, particularly at early post-exposure times. We therefore sought to explore a possibility that susceptible G₂ populations are formed by Cr-damaged cells that progressed through S-phase. To test this hypothesis, we scored the number of γ H2AX+ cells in the presence and absence of DNA polymerase inhibitor aphidicolin (Figure 6A–D). We found that aphidicolin strongly decreased the total number of γ H2AX+ cells in both HBE (Figure 6A and B) and IMR90 (Figure 6C and D) cells irrespective of their Asc status. The inhibitory effect of aphidicolin on DSB induction was even more striking for G₂ cells, which led to the complete absence of γ H2AX/cyclin B1 dual positive cells. It should be noted that the presence of aphidicolin diminished G₂ populations by \sim 2–2.5-fold (Figure 6E and F), which still left \sim 6–8% of cells that entered G₂ phase before addition of aphidicolin and Cr.

Since entry of Cr-damaged cells from S to G₂ phase had such a profound effect on the induction of γ H2AX, we also examined whether the differences in genotoxic responses between Asc+ and Asc- cells were associated with potentially varying rates of S to G₂ progression. To explore this possibility, we pulse-labeled replicating cells with BrdU prior to Cr treatments and then analyzed the appearance of BrdU-tagged DNA in G₂ phase by co-staining with anti-BrdU and anti-cyclin B1 antibodies. These experiments found that Asc had no effect on the rate of S to G₂ progression at 1–6 h post-Cr (Figure 6G and H), a time interval when Asc+ cells always had dramatically higher levels of γ H2AX (Figure 6, compare A versus B, C versus D). In accordance with the S-dependent sensitization of G₂ cells, the overall number of BrdU/B1 dual positive Asc+ cells roughly corresponded to the number of γ H2AX/B1 dual positive Asc+ cells (Figure 6, panels G and D).

DISCUSSION

Mechanism of Asc-promoted chromate genotoxicity

Our studies demonstrated that cellular Asc acted as a potent amplifier of clastogenic and mutagenic activities of carcinogenic Cr(VI). Potentiating effects of Asc were observed when it was present during Cr(VI) metabolism (preloading experiments) but no effects on clastogenic or mutagenic responses were detected when Asc was introduced following exposure and reduction of Cr(VI). Therefore, the targets of Asc were Cr(VI) metabolism and resulting DNA damage rather than cellular damage response mechanisms. Asc-promoted clastogenesis was not the result of the formation of some intrinsically more genotoxic damage, because the induction of DSB foci and micronuclei were almost completely suppressed by stable knockdowns of MSH2 or MLH1 MMR proteins. Thus, unrepaired chromosomal breaks were apparently caused by aberrant processing of Asc-promoted Cr-DNA damage by MMR proteins. Considering that Asc is the fastest biological reducer of Cr(VI) (10),

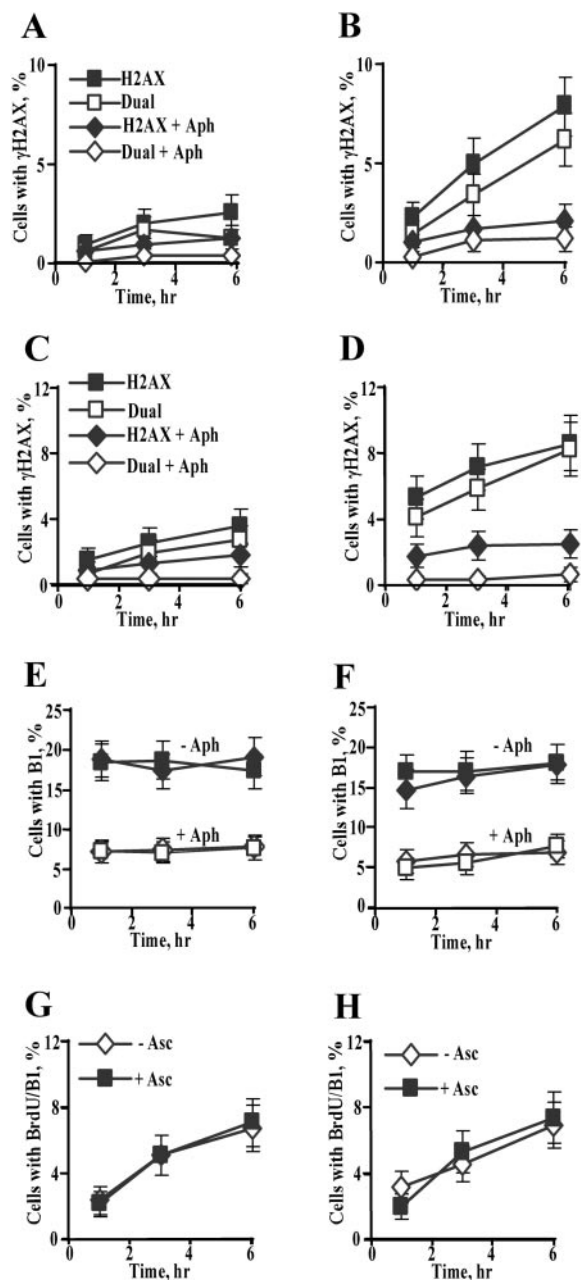


Figure 6. DNA polymerase inhibitor aphidicolin abolished induction of DSB in G₂ cells. All experiments were conducted with 3 μM Cr(VI) exposures for 3 h. Aphidicolin (1 μM) was added 15 min before Cr and was present during and after Cr exposures. Cells were fixed for immunostaining at 1, 3 and 6 h post-Cr treatments. Data are means ± SD for four slides with >100 cells/slide counted. (A) Effect of aphidicolin on frequency of total γH2AX+ (H2AX) and (B) γH2AX/cyclin B1 dual positive (dual) HBE cells lacking Asc, or (C) and (D) preloaded with 1.7 mM Asc. Panels A and B have the same legend. (C) Effect of aphidicolin on frequency of total γH2AX+ (H2AX) and γH2AX/cyclin B1 dual positive (dual) IMR90 cells lacking Asc, or (D) preloaded with 1 mM Asc. Panels C and D have the same legend. In untreated controls, frequency of γH2AX+ cells varied from 0.3 to 0.9% for IMR90 cells, and from 0.3 to 0.6% for HBE cells. (E) Percentage of cyclin B1-positive HBE and (F) IMR90 cells in the presence or absence of aphidicolin. Closed symbols—no aphidicolin (–Aph), open symbols—1 μM aphidicolin (+Aph); squares +Asc, diamonds –Asc. (G) Assessment of S to G₂ progression in Cr-treated or (H) untreated IMR90 cells containing or lacking Asc. Cells were labeled with 10 μM BrdU for 15 min prior to 3 μM Cr and fixed for immunostaining at 1, 3 and 6 h post-Cr. Data are means±SD for three slides with >100 cells counted per slide.

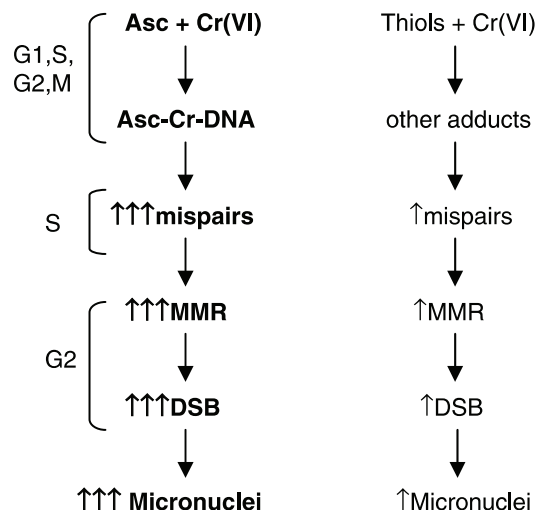


Figure 7. A model of Asc-promoted genotoxicity and mutagenicity of carcinogenic chromium(VI).

one of the direct consequences of Asc's presence is a more rapid reduction of Cr(VI) to stable Cr(III). This by itself may not be very important since Cr-DNA binding in cells was independent of the Asc status. A truly unique aspect of Cr(VI) metabolism by Asc is the formation of highly mutagenic Asc-Cr-DNA crosslinks (19,39). Thus, elevated mutagenic activity of Cr(VI) in CHO and V79 cells was probably a result of the formation of this premutagenic lesion. It is possible that other forms of DNA damage were also induced by Asc loading (40), although shuttle-vector experiments did not find evidence for a significant role of oxidative damage in mutagenic responses generated by Asc-Cr(VI) reactions *in vitro* (18,39). A consideration of the complete set of experimental findings leads us to propose a model of Asc-enhanced genotoxicity involving the formation of premutagenic Asc-Cr-DNA crosslinks (Figure 7). In this model, premutagenic Asc-Cr-DNA adducts generate a high frequency of base mispairs during DNA replication and the resulting compound lesions (Cr-DNA adducts containing mismatches) are recognized by MMR. This then leads to the aberrant processing and production of DSB in G₂ cells. Progression of G₂ cells with unrepaired DSB into mitosis would generate clastogenic events that were detected as kinetochore-negative micronuclei in our experiments. The same mechanism for the induction of DSB and micronuclei should also operate for Asc– cells with the exception that thiol-stimulated DNA damage is poorly mutagenic, which consequently should cause only weak base mispairing and mild activation of MMR. It is possible that S-phase creates favorable conditions for the direct detection of Asc-Cr-DNA adducts by MMR proteins although in the cases of other DNA adducts, compound lesions were always detected with much higher specificity (41,42).

Cr is not unique in its ability to activate genotoxicity in a MMR-dependent manner. It has been known for quite some time that toxicity of S_N1 methylating agents (MNNG, MNU and their clinical analogues) forming O⁶-methylguanine requires the presence of MMR proteins (43,44). Other examples of genotoxicants with MMR-mediated toxic responses include cisplatin and thiopurines (45,46). As with Cr, DNA

breaks were also implicated as secondary toxic lesions in cells treated with MNNG and 6-thioguanine. However, the induction of DNA breaks does not follow the same pattern for any two types of DNA damaging agents. For 6-thioguanine, MMR generated only single-strand breaks (SSB) even after two rounds of cell cycle (47) while processing of O⁶methyl-G produced SSB after the first S-phase and then DSB in the second S-phase (48). The formation of DSB in the second S-phase was proposed to result from the unavoidable termination of replication at the sites of SSB. While the formation of persistent SSB from repetitive cycles of MMR across highly mutagenic DNA lesions (futile repair cycling) would be expected, the induction of DSB in Cr-treated cells after the first round of replication is unprecedented and must originate from a different mechanism than breakage generation for other genotoxicants. Sensitivity of SSB repair deficient XRCC1^{-/-} and proficient XRCC1⁺ cells to low-moderate amounts of Cr-DNA damage has been found to be very similar (20), indicating that SSB are not important toxic lesions and consequently, that Cr-induced DSB did not result from the SSB to DSB conversion sequence. We favor a possibility that DSB in Cr-treated cells are caused by collapsed replication forks. In this scenario, assembly of MMR complexes at the sites of Cr-DNA damage or Cr-induced mismatches stalls replication forks that remain intact as long as cells remain in S-phase. Transition of cells from S to G₂ inactivates fork viability mechanisms resulting in collapsed forks, which are known to result in the generation of DSB (49,50).

Implications for chromium carcinogenesis

We have recently proposed that occupational Cr carcinogenesis may involve selection of Cr-resistant, MMR-deficient cells (36,51). This selection model was based on a MMR-dependent mechanism of apoptosis in Cr(VI)-treated cells (36) and is further supported by a high frequency of microsatellite instability (52) and the loss of MLH1 expression in lung cancers among chromate workers (53). The selection process is expected to operate most efficiently at toxic, repetitive exposures. Suppression of DNA DSB and micronuclei formation by subtoxic exposures in cells with stable knockdowns of MLH1 or MSH2 indicates that MMR can also promote carcinogenesis by environmental doses of Cr via potentiation of chromosomal instability. Taken together, these results suggest that MMR plays a major role in the cellular responses to Cr over a broad range of doses and therefore, it may represent an important factor in the individual susceptibility to genetic damage in Cr-exposed populations.

A key mechanistic difference in Cr(VI) reduction by Asc relative to other reducers is the absence of Cr(V) intermediate under physiologically relevant conditions (16,17). The formation of Cr(V) was only detectable when Cr(VI) was present in equimolar or excess amounts over Asc concentrations, experimental conditions that would approximate rare massive human exposures to Cr(VI). Although it has been previously suggested that Cr(V) could be an important DNA-reactive intermediate, highly elevated genotoxic and mutagenic responses in Asc-containing cells treated with low to moderate doses of Cr strongly argue against any major biological role

of Cr(V). In fact, further channeling of Cr(VI) into Cr(V)-skipping metabolism by increasing cellular levels of Asc caused progressively more genetic damage. The same conclusion was also drawn from *in vitro* studies on the formation of mutagenic DNA damage in Cr(VI)-Asc reactions (18,39). These mechanistic considerations predict that DNA damage induction should be a linear or near linear function of cellular Cr doses, which is what we found for Cr-DNA binding and biological indices of genotoxicity, such as DSB, micronuclei and mutagenesis. Thus, our studies did not find any support for the notion that there is a safe range of Cr doses, resulting from the suppression of Cr(V) formation by Asc. Overall, our results raise a possibility that consumption of large amounts of vitamin C accompanied by its high tissue accumulation could in fact exacerbate genetic damage of Cr(VI) exposures. This scenario would resemble a situation with another metal-caused disease, hemochromatosis, the dietary management of which includes a recommendation of avoiding excess vitamin C to decrease redox cycling of iron (54).

ACKNOWLEDGEMENTS

This work was supported by NIH research grants ES008786, ES012915 and training grant ES007272. We thank Elizabeth Bartley for the critical reading of the manuscript and many helpful suggestions. Funding to pay the Open Access publication charges for this article was provided by NIEHS.

Conflict of interest statement. None declared.

REFERENCES

- Langard,S. (1990) One hundred years of chromium and cancer: a review of epidemiological evidence and selected case reports. *Am. J. Ind. Med.*, **17**, 189–215.
- Sorahan,T., Burges,D.C., Hamilton,L. and Harrington,J.M. (1998) Lung cancer mortality in nickel/chromium platers, 1946–1995. *Occup. Environ. Med.*, **55**, 236–242.
- Pellerin,C. and Booker,S.M. (2000) Reflections on hexavalent chromium: health hazards of an industrial heavyweight. *Environ. Health Perspect.*, **108**, A402–A407.
- Zhitkovich,A. (2002) Chromium: exposure, toxicity and biomonitoring approaches. In Wilson,S.H. and Suk,W.A. (eds), *Biomarkers of Environmentally Associated Disease: Technologies, Concepts, and Perspective*. CRC Press LLC, New York, pp. 269–287.
- De Flora,S. (2000) Threshold mechanisms and site specificity in chromium(VI) carcinogenesis. *Carcinogenesis*, **21**, 533–541.
- Cohen,M.D., Kargacin,B., Klein,C.B. and Costa,M. (1993) Mechanisms of chromium carcinogenicity and toxicity. *Crit. Rev. Toxicol.*, **23**, 255–281.
- Gibb,H.J., Lees,P.S.J., Pinsky,P.F. and Rooney,B.C. (2000) Lung cancer among workers in chromium chemical production. *Am. J. Ind. Med.*, **38**, 115–126.
- Park,R.M., Bena,J.F., Stayner,L.T., Smith,R.J., Gibb,H.J. and Lees,P.S. (2004) Hexavalent chromium and lung cancer in the chromate industry: a quantitative risk assessment. *Risk Anal.*, **24**, 1099–1108.
- Occupational Safety and Health Administration (OSHA), Department of Labor. (2006) Occupational exposure to hexavalent chromium. Final rule. *Fed. Regist.*, **71**, 10099–10385.
- Zhitkovich,A. (2005) Importance of chromium-DNA adducts in mutagenicity and toxicity of chromium(VI). *Chem. Res. Toxicol.*, **18**, 3–11.
- Levina,A. and Lay,P.A. (2005) Mechanistic studies of relevance to the biological activities of chromium. *Coord. Chem. Rev.*, **249**, 281–298.

12. Shi, H., Hudson, L.G. and Liu, K.J. (2004) Oxidative stress and apoptosis in metal ion-induced carcinogenesis. *Free Radic. Biol. Med.*, **37**, 582–593.
13. Sugden, K.D., Campo, C.K. and Martin, B.D. (2001) Direct oxidation of guanine and 7,8-dihydro-8-oxoguanine in DNA by a high-valent chromium complex: a possible mechanism for chromate genotoxicity. *Chem. Res. Toxicol.*, **14**, 1315–1322.
14. Levina, A., Barr-David, G., Codd, R., Lay, P.A., Dixon, N.E., Hammershoi, A. and Hendry, P. (1999) *In vitro* plasmid DNA cleavage by chromium(V) and -(IV) 2-hydroxycarboxylate complexes. *Chem. Res. Toxicol.*, **12**, 371–381.
15. Standeven, A.M. and Wetterhahn, K.E. (1992) Ascorbate is the principal reductant of chromium(VI) in rat lung ultrafiltrates and cytosols, and mediates chromium-DNA binding *in vitro*. *Carcinogenesis*, **13**, 1319–1324.
16. Stearns, D.M. and Wetterhahn, K.E. (1994) Reaction of Cr(VI) with ascorbate produces chromium(V), chromium(IV), and carbon-based radicals. *Chem. Res. Toxicol.*, **7**, 219–230.
17. Lay, P.A. and Levina, A. (1998) Activation of molecular oxygen during the reactions of chromium(VI/IV) with biological reductants: implications for chromium-induced genotoxicities. *J. Am. Chem. Soc.*, **120**, 6704–6714.
18. Quievryn, G., Messer, J. and Zhitkovich, A. (2006) Lower mutagenicity but higher stability of Cr-DNA adducts formed during gradual chromate activation with ascorbate. *Carcinogenesis*, **27**, 2316–2321.
19. Quievryn, G., Messer, J. and Zhitkovich, A. (2002) Carcinogenic chromium(VI) induces cross-linking of vitamin C to DNA *in vitro* and in human lung A549 cells. *Biochemistry*, **41**, 3156–3167.
20. Messer, J., Reynolds, M., Stoddard, L. and Zhitkovich, A. (2006) Causes of DNA single-strand breaks during reduction of chromate by glutathione *in vitro* and in cells. *Free Radic. Biol. Med.*, **40**, 1981–1992.
21. Luo, Y., Lin, F.T. and Lin, W.C. (2004) ATM-mediated stabilization of hMutL DNA mismatch repair proteins augments p53 activation during DNA damage. *Mol. Cell. Biol.*, **24**, 6430–6434.
22. Reynolds, M., Peterson, E., Quievryn, G. and Zhitkovich, A. (2004) Human nucleotide excision repair efficiently removes DNA phosphate-chromium adducts and protects cells against chromate toxicity. *J. Biol. Chem.*, **279**, 30419–30424.
23. Karaczyn, A., Ivanov, S., Reynolds, M., Zhitkovich, A., Kasprzak, K.S. and Salnikow, K. (2006) Ascorbate depletion mediates up-regulation of hypoxia-associated proteins by cell density and nickel. *J. Cell. Biochem.*, **97**, 1025–1035.
24. Guaiquil, V.H., Farber, C.M., Golde, D.W. and Vera, J.C. (1997) Efficient transport and accumulation of vitamin C in HL-60 cells depleted of glutathione. *J. Biol. Chem.*, **272**, 9915–9921.
25. Koh, W.S., Lee, S.J., Lee, H., Park, C., Park, M.H., Kim, W.S., Yoon, S.S., Park, K., Hong, S.I., Chung, M.H. and Park, C.H. (1998) Differential effects and transport kinetics of ascorbate derivatives in leukemic cell lines. *Anticancer Res.*, **18**, 2487–2493.
26. Rogakou, E.P., Pilch, D.R., Orr, A.H., Ivanova, V.S. and Bonner, W.M. (1998) DNA double-stranded breaks induce histone H2AX phosphorylation on serine 139. *J. Biol. Chem.*, **273**, 5858–5868.
27. Rogakou, E.P., Boon, C., Redon, C. and Bonner, W.M. (1999) Megabase chromatin domains involved in DNA double-strand breaks *in vivo*. *J. Cell. Biol.*, **146**, 905–916.
28. Wang, Z.Q., Stingl, L., Morrison, C., Jantsch, M., Los, M., Schulze-Osthoff, K. and Wagner, E.F. (1997) PARP is important for genomic stability but dispensable in apoptosis. *Genes Dev.*, **11**, 2347–2358.
29. Kirsch-Volders, M., Sofuni, T., Aardema, M., Albertini, S., Eastmond, D., Fenech, M., Ishidate, M., Jr, Kirchner, S., Lorge, E., Morita, T. *et al.* (2003) Report from the *in vitro* micronucleus assay working group. *Mutat. Res.*, **540**, 153–163.
30. Schultz, L.B., Chehab, N.H., Malikzay, A. and Halazonetis, T.D. (2000) p53 binding protein 1 (53BP1) is an early participant in the cellular response to DNA double-strand breaks. *J. Cell. Biol.*, **151**, 1381–1390.
31. Celeste, A., Fernandez-Capetillo, O., Kruhlak, M.J., Pilch, D.R., Staudt, D.W., Lee, A., Bonner, R.F., Bonner, W.M. and Nussenzweig, A. (2003) Histone H2AX phosphorylation is dispensable for the initial recognition of DNA breaks. *Nature Cell. Biol.*, **5**, 675–679.
32. Mochan, T.A., Venere, M., DiTullio, R.A., Jr and Halazonetis, T.D. (2004) 53BP1, an activator of ATM in response to DNA damage. *DNA Repair (Amst.)*, **3**, 945–952.
33. Aaron, C.S., Bolcsfoldi, G., Glatt, H.R., Moore, M., Nishi, Y., Stankowski, L., Theiss, J. and Thompson, E. (1994) Mammalian cell gene mutation assays working group report. *Mutat. Res.*, **312**, 235–239.
34. Dillon, C.T., Lay, P.A., Bonin, A.M., Dixon, N.E., Collins, T.J. and Kostka, K.L. (1997) Microprobe X-ray absorption spectroscopic determination of the oxidation state of intracellular chromium following exposure of V79 Chinese hamster lung cells to genotoxic chromium complexes. *Chem. Res. Toxicol.*, **10**, 533–535.
35. Wei, Y.D., Tepperman, K., Huang, M.Y., Sartor, M.A. and Puga, A. (2004) Chromium inhibits transcription from polycyclic aromatic hydrocarbon-inducible promoters by blocking the release of histone deacetylase and preventing the binding of p300 to chromatin. *J. Biol. Chem.*, **279**, 4110–4119.
36. Peterson-Roth, E., Reynolds, M., Quievryn, G. and Zhitkovich, A. (2005) Mismatch repair proteins are activators of toxic responses to chromium-DNA damage. *Mol. Cell. Biol.*, **25**, 3596–3607.
37. Kunkel, T.A. and Erie, D.A. (2005) DNA mismatch repair. *Annu. Rev. Biochem.*, **74**, 681–710.
38. Modrich, P. (2006) Mechanisms in eukaryotic mismatch repair. *J. Biol. Chem.*, **281**, 30305–30309.
39. Quievryn, G., Peterson, E., Messer, J. and Zhitkovich, A. (2003) Genotoxicity and mutagenicity of chromium(VI)/ascorbate-generated DNA adducts in human and bacterial cells. *Biochemistry*, **42**, 1062–1070.
40. Slade, P.G., Hailer, M.K., Martin, B.D. and Sugden, K.D. (2005) Guanine-specific oxidation of double-stranded DNA by Cr(VI) and ascorbic acid forms spiroiminodihydroantoin and 8-oxo-2'-deoxyguanosine. *Chem. Res. Toxicol.*, **18**, 1140–1149.
41. Fourrier, L., Brooks, P. and Malinge, J.-M. (2003) Binding discrimination of MutS to a set of lesions and compound lesions (base damage and mismatch) reveals its potential role as a cisplatin-damaged DNA sensing protein. *J. Biol. Chem.*, **278**, 21267–21275.
42. Yoshioka, K.-I., Yoshioka, Y. and Hsieh, P. (2006) ATR kinase activation mediated by MutS α and MutL α in response to cytotoxic O⁶-methylguanine adducts. *Mol. Cell*, **22**, 501–510.
43. Bignami, M., O'Driscoll, M., Aquilina, G. and Karran, P. (2000) Unmasking a killer: DNA O(6)-methylguanine and the cytotoxicity of methylating agents. *Mutat. Res.*, **462**, 71–82.
44. Kaina, B. (2004) Mechanisms and consequences of methylating agent-induced SCEs and chromosomal aberrations: a long road traveled and still a far way to go. *Cytogenet. Genome Res.*, **104**, 77–86.
45. Papouli, E., Cejka, P. and Jiricny, J. (2004) Dependence of the cytotoxicity of DNA-damaging agents on the mismatch repair status of human cells. *Cancer Res.*, **64**, 3391–3394.
46. Massey, A., Xu, Y.Z. and Karran, P. (2001) Photoactivation of DNA thiobases as a potential novel therapeutic option. *Curr. Biol.*, **11**, 1142–1146.
47. Yan, T., Berry, S.E., Desai, A.B. and Kinsella, T.J. (2003) DNA mismatch repair (MMR) mediates 6-thioguanine genotoxicity by introducing single-strand breaks to signal a G₂-M arrest in MMR-proficient RKO cells. *Clin. Cancer Res.*, **9**, 2327–2334.
48. Stojic, L., Mojas, N., Cejka, P., Di Pietro, M., Ferrari, S., Marra, G. and Jiricny, J. (2004) Mismatch repair-dependent G₂ checkpoint induced by low doses of SN1 type methylating agents requires the ATR kinase. *Genes Dev.*, **18**, 1331–1344.
49. Courcelle, J., Donaldson, J.R., Chow, K.H. and Courcelle, C.T. (2003) DNA damage-induced replication fork regression and processing in *Escherichia coli*. *Science*, **299**, 1064–1067.
50. Sogo, J.M., Lopes, M. and Foiani, M. (2002) Fork reversal and ssDNA accumulation at stalled replication forks owing to checkpoint defects. *Science*, **297**, 599–602.
51. Zhitkovich, A., Peterson-Roth, E. and Reynolds, M. (2005) Killing of chromium-damaged cells by mismatch repair and its relevance to carcinogenesis. *Cell Cycle*, **4**, 1050–1052.
52. Hirose, T., Kondo, K., Takahashi, Y., Ishikura, H., Fujino, H., Tsuyuguchi, M., Hashimoto, M., Yokose, T., Mukai, K.,

- Kodama, T. *et al.* (2002) Frequent microsatellite instability in lung cancer from chromate-exposed workers. *Mol. Carcinog.*, **33**, 172–180.
53. Takahashi, Y., Kondo, K., Hirose, T., Nakagawa, H., Tsuyuguchi, M., Hashimoto, M., Sano, T., Ochiai, A. and Monden, Y. (2005) Microsatellite instability and protein expression of the DNA mismatch repair gene, hMLH1, of lung cancer in chromate-exposed workers. *Mol. Carcinog.*, **42**, 150–158.
54. Barton, J.C., McDonnell, S.M., Adams, P.C., Brissot, P., Powell, L.W., Edwards, C.Q., Cook, J.D. and Kowdley, K.V. (1998) Management of hemochromatosis. Hemochromatosis management working group. *Ann. Intern. Med.*, **129**, 932–939.